Synthesis and Photophysical Properties of Thioglycosylated Chlorins, Isobacteriochlorins, and Bacteriochlorins for Bioimaging and Diagnostics

ARTICLE *in* BIOCONJUGATE CHEMISTRY · OCTOBER 2010

Impact Factor: 4.51 · DOI: 10.1021/bc100356z · Source: PubMed

9 AUTHORS, INCLUDING:

Amit Aggarwal
City University of New York - LaGuardia Co…
24 PUBLICATIONS **147** CITATIONS
SEE PROFILE

Sebastian Thompson
ICFO Institute of Photonic Sciences
10 PUBLICATIONS **232** CITATIONS
SEE PROFILE

Charles Michael Drain
City University of New York - Hunter College
118 PUBLICATIONS **3,927** CITATIONS
SEE PROFILE

Synthesis and Photophysical Properties of Thioglycosylated Chlorins, Isobacteriochlorins, and Bacteriochlorins for Bioimaging and Diagnostics

Sunaina Singh,[†] Amit Aggarwal,[†] Sebastian Thompson,[†] João P. C. Tomé,[†] Xianchun Zhu,[‡] Diana Samaroo,[#] Mikki Vinodu,[†] Ruomei Gao,[‡] and Charles Michael Drain[†,§,*]

Department of Chemistry & Biochemistry, Hunter College of the City University of New York, 695 Park Avenue, New York, New York 10065, United States, Department of Chemistry and Biochemistry, Jackson State University, 1400 J. R. Lynch Street, Jackson, Mississippi 39217, United States, NYC College of Technology, 300 Jay Street, Brooklyn, New York 11201, United States, and The Rockefeller University, 1230 York Avenue, New York, New York 10065, United States. Received August 4, 2010; Revised Manuscript Received September 23, 2010

The facile synthesis and photophysical properties of three nonhydrolyzable thioglycosylated porphyrinoids are reported. Starting from *meso*-perfluorophenylporphyrin, the nonhydrolyzable thioglycosylated porphyrin ($PGlc_4$), chlorin ($CGlc_4$), isobacteriochlorin ($IGlc_4$), and bacteriochlorin ($BGlc_4$) can be made in 2−3 steps. The ability to append a wide range of targeting agents onto the perfluorophenyl moieties, the chemical stability, and the ability to fine-tune the photophysical properties of the chromophores make this a suitable platform for development of biochemical tags, diagnostics, or as photodynamic therapeutic agents. Compared to the porphyrin in phosphate buffered saline, $CGlc_4$ has a markedly greater absorbance of red light near 650 nm and a 6-fold increase in fluorescence quantum yield, whereas $IGlc_4$ has broad Q-bands and a 12-fold increase in fluorescence quantum yield. $BGlc_4$ has a similar fluorescence quantum yield to $PGlc_4$ (<10%), but the lowest-energy absorption/emission peaks of $BGlc_4$ are considerably red-shifted to near 730 nm with a nearly 50-fold greater absorbance, which may allow this conjugate to be an effective PDT agent. The uptake of $CGlc_4$, $IGlc_4$, and $BGlc_4$ derivatives into cells such as human breast cancer cells MDA-MB-231 and K:Molv NIH 3T3 mouse fibroblast cells can be observed at nanomolar concentrations. Photobleaching under these conditions is minimal.

INTRODUCTION

Chlorins are porphyrinoids with one pyrrole double bond missing. Isobacteriochlorins and bacteriochlorins are porphyrinoids with two pyrrole double bonds missing on adjacent or opposite pyrroles, respectively. Oxidative or reductive transformations of porphyrins can yield these chromophores. Porphyrins, chlorins, bacteriochlorins, and isobacteriochlorins each have unique photophysical properties that are exploited by nature and can be used for diverse applications (*1, 2*). Compared to the parent tetraarylporphyrin, the intensity of the lowest-energy UV−visible absorption band near 650 nm can increase by ∼20-fold for chlorins and by ∼5-fold for the isobacteriochlorins. For bacteriochlorins, the absorption band near 650 nm is similar to porphyrins, but an additional high-intensity absorption band appears near 730 nm. The excited-state lifetimes, singlet and triplet quantum yields, and distortion upon metal ion binding are significantly different for these three types of macrocycles (*3, 4*).

For diagnostic and photodynamic therapeutic (PDT) applications, the enhanced intensity of the low-energy absorption bands allows more efficient use of wavelengths of light that penetrate further into tissues (*5*−*8*). An example of a chlorin PDT photosensitizer is *meso*-tetrakis(3′-hydroxyphenyl)chlorin (m-THPC) and its derivatives (*9*). Other water-soluble chlorins are reported (*10*−*12*). For therapeutic uses of PDT agents, high triplet quantum yields are desirable to photosensitize the formation of singlet oxygen and other reactive oxygen species, which then cause damage to diverse cellular components. For diagnostics, the dyes appended with appropriate targeting motifs need to have greater fluorescence quantum yields for use as fluorescent tags or trackers (*13*). Fluorescent dyes with targeting motifs can be used in fluorescence guided surgery (*14*).

Porphyrins, chlorins, isobacteriochlorins, bacteriochlorins, and phthalocyanines with 1−8 appended sugar moieties can have cytotoxic activity, because the sugars can direct the chromophore to some cancer cells (*15*−*27*). However, most reported compounds have O-glyco linkages where hydrolysis may diminish in vivo effectiveness compared to corresponding nonhydrolyzable derivatives. The number, type, and position of the sugar moieties have long been known to effect cell uptake and photochemical properties (*16, 21, 28*). The synthesis of a polyglycerol dendrimer with a porphyrin core is reported (*29*), click reactions have been used to glycosylate chlorin e_6 (*30*), and polysaccharides have been appended to porphyrins (*31*).

Previously, we reported the synthesis of nonhydrolyzable thioglycosylated tetraarylporphyrins and showed that the tetraglucose derivative ($PGlc_4$, Scheme 1, **1b**) is a selective and effective PDT agent in vitro using several cell lines, such as MDA-MB-231 human breast cancer cells, whereas the galactose derivative is much less effective (*32*). Also, the glycosylated compounds were taken up by transformed mouse $3Y1^{vSrc}$ cells but not taken up by normal mouse fibroblast cells (*32, 33*). We first reported the synthesis and ground-state electronic properties of a glycosylated chlorin formed using a dipolar addition to $TPPF_{20}$ to append a fused *N*-methyl-pyrrolidine moiety and the same chemistry to append the sugars (Scheme 2) (*34*).

One advantage of using the tetraperfluorophenylporphyrin ($TPPF_{20}$) is that it can serve as a core platform for a host of materials (*35, 36*) and biochemical applications because the para fluoro group can be routinely substituted with a variety of

* To whom correspondence should be addressed. (C.M.D.) Phone: 212-650-3791. Fax: 212-772-5332. E-mail: cdrain@hunter.cuny.edu.
[†] Hunter College.
[‡] Jackson State University.
[#] New York City College of Technology.
[§] Rockefeller University.

10.1021/bc100356z
Published on Web 10/21/2010

Scheme 1. Synthesis of $PGlc_4$ from Tetrakis(pentafluorophenyl)porphyrin ($TPPF_{20}$)

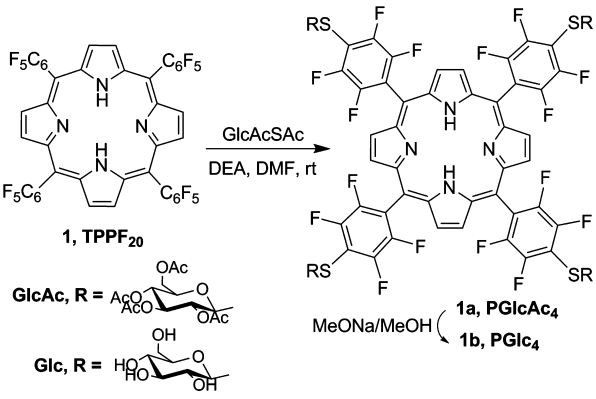

nucleophiles to form bioconjugates, biocompatible compounds, and combinatorial libraries (*33, 37*−*41*). For example, we have appended ethylene glycols, polyamines, lysines, alkanes, fluorous alkanes, sugars, and nucleotides using both primary amines and thiols. Subsequently, glycols with an oxygen linkage were also reported (*42*). The PDT activity of many of these derivatives has been studied with a variety of cell lines, and the glycosylated compounds affect apoptosis in several cases (*22, 42*−*44*). Also, the 16 fluoro groups make this compound amenable for in vivo ^{19}F NMR studies of localization (*45*).

Given the diversity of the targeting moieties on the core platform, it is desirable to be able to tune the photophysical properties of the chromophore for these assorted applications, and an obvious means to accomplish this is to adjust the number of double bonds in the macrocycle as is done in nature (*46*). There are many strategies to make porphyrins lacking one or two double bonds using oxidative and reductive strategies (*5, 47*). The formation of the perfluorophenylchlorin (CF_{20}), perfluorophenylisobacteriochlorin (IF_{20}), and perfluorophenylbacteriochlorin (BF_{20}) by 1,3-dipolar additions was reported by the Cavaleiro group (*48*−*52*). The advantage of this route is that it does not use toxic reagents and the products are reasonably stable chemically and to photobleaching. Vicente and co-workers exploited the thio coupling chemistry on CF_{20} to append carboranyl groups (*53*), and Hirohara has appended sugars to free base and Pt derivatives (*54, 55*) for potential therapeutic applications. We now report the synthesis, photophysical properties, and relative cell uptake of the glycosylated chlorin **2b** ($CGlc_4$), isobacteriochlorin **3b** ($IGlc_4$), and bacteriochlorin **4b** ($BGlc_4$) analogues (Scheme 2).

EXPERIMENTAL PROCEDURE

Materials and Methods. *General.* ^1H and ^{13}C NMR spectra were recorded in a Brüker Avance 500 MHz spectrometer and the ^{19}F spectra in a JEOL 400 MHz spectrometer. Electrospray ionization mass spectrometric analyses were performed at the CUNY Mass Spectrometry Facility at Hunter College using an Agilent Technologies HP-1100 LC/MSD instrument. The electrospray ionization was run in methanol, with 0.1% formic acid. UV-visible spectra were recorded on a Varian Bio3 spectrophotometer. Steady-state fluorescence (emission) spectra were measured with a Fluorolog τ3, Jobin-SPEX Instruments S.A., Inc. All reagents were obtained from commercial sources and used without further purification. $TPPF_{20}$ porphyrin was obtained from Frontier Scientific. Dulbecco's Modified Eagle Medium (DMEM), trypsin-EDTA, and antimycotic for cell culture were obtained from GibcoBRL. Hanks' balanced salt solution was obtained from Cellgro (Mediatech). Bovine calf serum was obtained from HyClone. Phosphate buffered saline (PBS) was purchased from Invitrogen. Flash column chromatography was performed using silica gel-60, and the analytical TLC was carried out on precoated sheets with silica gel (0.2 mm thick), both from Sorbent Technologies. The octanol/water partition coefficients were determined by saturating 1:1 (v/v) mixtures of the solvents with the porphyrinoid, waiting 8−10 h, and measuring the Soret and first Q-band intensities. This data were confirmed by saturating each solvent separately before mixing equal volumes.

Synthesis. *Improved Synthesis $PGlcAc_4$ (**1a**).* To a solution of $TPPF_{20}$, **1** (50 mg, 51 μmol), and 2,3,4,6-tetra-*O*-acetylglucosylthioacetate (90 mg, 233 μmol, 4.6 equiv) in DMF (5 mL), diethyl amine (1 mL) was added. The reaction mixture was stirred at room temperature for 1.5 h. Then, the product was precipitated with methanol/water and the solid filtered through a short column of Celite and washed with water. The crude mixture was recovered in dichloromethane and purified by flash chromatography (silica gel) using a mixture of ethyl acetate/hexanes (3:1) as eluent. The glycoporphyrin **1a** (110 mg, 92%) was obtained after crystallization in dichloromethane/hexane, as a red powder.

*Synthesis of Porphyrin $PGlc_4$ (**1b**).* Porphyrin **1a** (50 mg, 21 μmol) was dissolved in methanol/dichloromethane (3:1, 8 mL) and treated with sodium methoxide (0.5 M solution in methanol, 1 mL). The reaction mixture was stirred at room temperature for 1.5 h and then neutralized by an aqueous citric acid solution. The mixture was filtered through a Waters Sep-Pak C_{18} 35 cm^3 reverse-phase prep column and washed with water. The deprotected glycoporphyrin **1b** was then purified on flash chromatography (silica gel) eluted using a mixture of ethyl acetate/methanol (3:1) and crystallized in methanol/CH_2Cl_2 (33.5 mg, 96%). mp > 250 °C. ^{19}F NMR (DMSO-d_6): δ −133.82 to −132.57 (m, 8F, Ar-*m*-F), −139.75 to −139.50 (m, 8F, Ar-*o*-F). ^1H NMR (DMSO-d_6): δ 9.33 (bs, 8H, pyrrolic β-H), 5.78 (bs, 4H, Glc-H), 5.10−5.29 (m, 13H, Glc-H), 4.72 (bs, 4H, Glc-H), 3.82−3.84 (m, 5H, Glc-H), 3.52−3.55 (m, 6H, Glc-H), 3.18−3.23(m, 12H, Glc-H), −3.17 (s, 2H, NH).

*Synthesis of Protected Thioglycosylated Chlorin, $CGlcAc_4$ (**2a**).* Chlorin **2** was prepared as previously reported method (*48, 49*). To a solution of chlorin **2** (25 mg, 24 μmol) and 2,3,4,6-tetra-*O*-acetyl-glucosylthioacetate (42 mg, 109 μmol, 4.5 equiv) in DMF (2.5 mL) diethyl amine (0.5 mL) was added. The reaction mixture was stirred at room temperature for 1 h. Then, the reaction mixture was precipitated with methanol/water, and the solid was filtered through a short column of Celite and washed with water. The crude mixture was recovered in CH_2Cl_2 and purified by flash chromatography (silica gel) using a mixture of ethyl acetate/hexanes (3:2) as eluent. Chlorin **2a** (48 mg, 82%) was obtained after crystallization in CH_2Cl_2 /hexanes, as a green powder. Because the *N*-methyl-pyrrolidine points to one face of the chlorin and the stereo centers on the sugars, **2a** is made as a mixture of diastereomers at the β-pyrrole positions bearing the *N*-methyl-pyrrolidine moieties. These are seen in some of the resonances in the ^1H NMR and especially the complexity of the phenyl region of the ^{13}C NMR, which show the coupling to ^{19}F and the diastereomers. The peaks in the ^{19}F NMR spectrum are somewhat broader than the achiral starting material. mp > 250 °C. ^{19}F NMR (DMSO-d_6): δ −130.09 to −129.81, −130.56 to −130.25 (2m, 4F, Ar-*m*-F), −131.69 to −131.54 (m, 4F, Ar-*m*-F), −137.10 to −136.78 (m, 2F, Ar-*o*-F), −138.98 to −138.82 (m, 6F, Ar-*o*-F). ^1H NMR ($CDCl_3$): δ 8.82−8.84, 8.55−8.57, 8.48−8.50 (3m, 6H, pyrrolic β-H), 5.11−5.40 (3m, 18H, 2H β-H [C (sp^3)] and 16H, Glc-H), 4.26−4.35 (m, 8H, Glc-H), 3.88−3.91 (m, 4H, Glc-H), 2.58 and 3.16 (2t, 4H, pyrrolidine-H), 2.22 (s, 3H, NCH_3), 2.07−2.10 (m, 48H, acetyl-H), −1.74 (s, 2H, NH). ^{13}C NMR ($CDCl_3$): δ 20.6 and 20.7 (CH_3CO_2), 41.2 (NCH_3), 53.1 and 53.2 (C2 and C3), 61.7 and 61.9 (Glc), 63.0 (CH_2), 68.0, 68.1, 70.7, 73.9, 84.5 and 84.6

Scheme 2. Synthesis of $CGlc_4$, $IGlc_4$, and $BGlc_4$

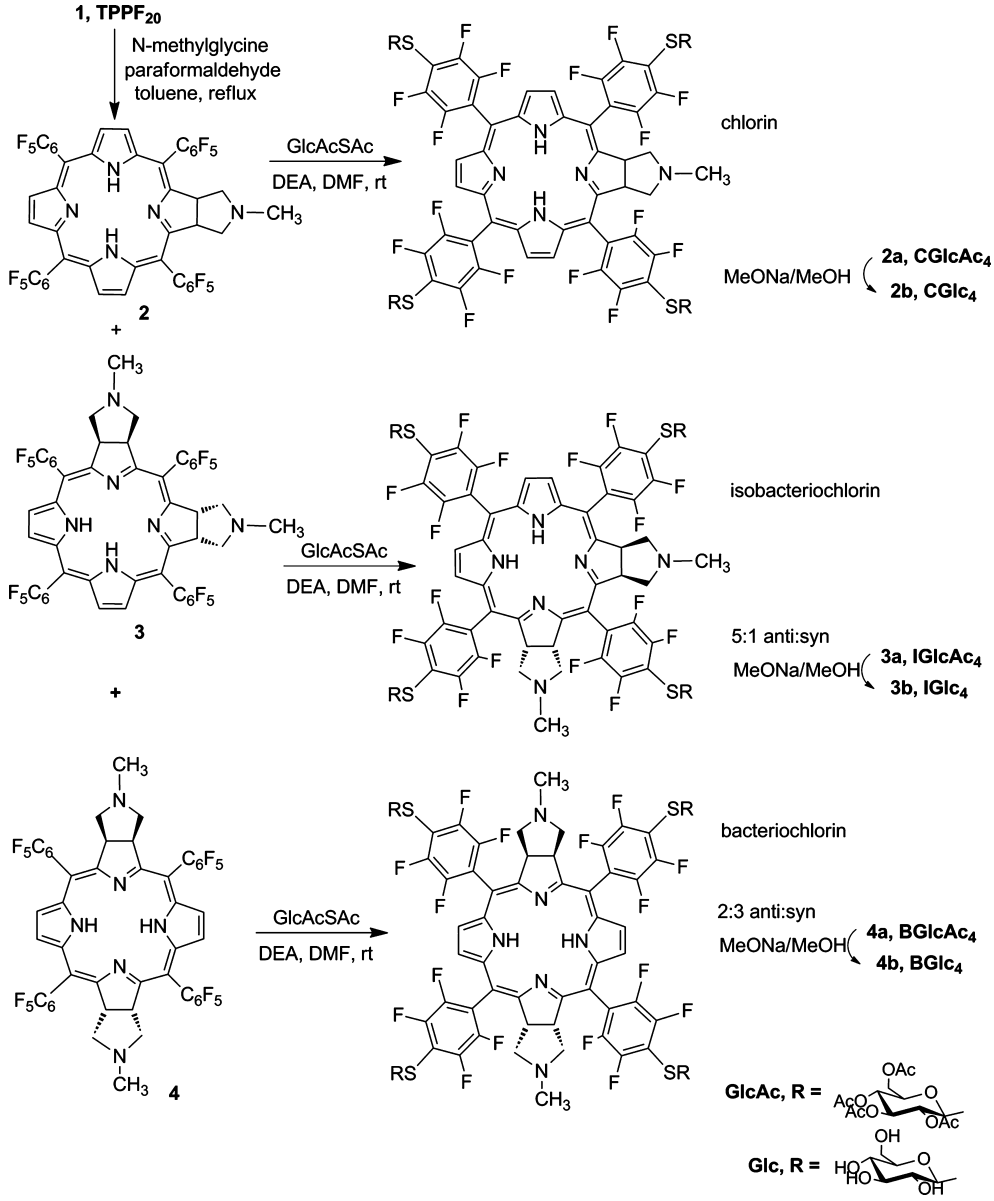

(Glc), 97.5, 106.7, 106.8, 111.6, 111.8, 122.1, 122.4, 124.0, 124.3, 128.2, 128.3, 132.5, 134.9, 135.0, 140.0, 141.1, 144−149 (C_6F_4), 152.3, 168.6, 168.8, 169.4 (CH_3CO_2), 170.2 and 170.7 (CH_3CO_2). HRMS calcd for $C_{103}H_{95}F_{16}N_5O_{36}S_4$ $(M+2H)^+$ 2409.4384, found 2409.4318.

*Synthesis of Thioglycosylated Chlorin, $CGlc_4$ (**2b**).* This details what we previously reported (*34*) and was later modified by Hirohara et al (*54*). Glycochlorin **2a** (30 mg, 12.4 μmol) was dissolved in methanol/CH_2Cl_2 (3:1, 4 mL) and treated with sodium methoxide (0.5 M solution in methanol, 1 mL). The reaction mixture was stirred at room temperature for 1 h and then neutralized by an aqueous citric acid solution. The mixture is filtered through Waters Sep-Pak C_{18} 35 cm^3 reverse-phase prep column and washed with water. The deprotected glycochlorin **2b** was then eluted with methanol and purified by flash chromatography (silica gel) using a mixture of ethyl acetate/methanol (3:2) as eluent. Chlorin **2b** (20 mg, 93%) was obtained after crystallization in methanol/CH_2Cl_2, as a green powder. **2b** is also a mixture of diastereomers. These are not well-resolved in the ^{1}H NMR but are observed, especially the complexity of the phenyl region of the ^{13}C NMR, which shows the coupling to ^{19}F and the diastereomers. mp > 250 °C. ^{19}F NMR (DMSO-d_6): δ −132.67 to −132.28 (m, 4F, Ar-*m*-F), −133.79 to −133.64 (m, 4F, Ar-*m*-F), −137.90 to −137.53 (m, 2F, Ar-*o*-F), −139.93 to −139.82 (m, 6F, Ar-*o*-F). ^{1}H NMR (DMSO-d_6): δ 9.14, 8.81 and 8.74 (3bs, 6H, pyrrolic β-H), 5.02−5.10, 5.28 and 5.75 (1m and 2bs, 18H, 2H β-H [C (sp^3)] and 16H, Glc-H), 4.55−4.68 (m, 4H, Glc-H), 4.10 (m, 2H, Glc-H), 3.73−3.78, 3.51, 3.18 and 3.04 (1m and 3bs, 26H, 4H pyrrolidine-H and 22H Glc-H), 2.05 (s, 3H, NCH_3), −1.97 (s, 2H, NH). ^{13}C NMR (DMSO-d_6): δ 41.0 (NCH_3), 49.1 and 53.1 (C2 and C3), 61.7, 61.71, and 61.9 (Glc), 62.9 (CH_2), 70.57, 70.60, 70.68, 70.78, 70.8, 75.1, 75.2, 78.51, 78.54, 78.6, 79.6, 82.2, 82.3, 84.9, 85.0 and 85.2 (Glc), 97.8, 106.8, 113.8, 113.9, 114.1, 114.2, 119.5, 119.6, 119.8, 120.0, 120.2, 126.6, 129.8, 133.5, 135.1, 140.3, 143−149 (C_6F_4), 152.4, 170.2. HRMS calcd. for $C_{71}H_{62}F_{16}N_5O_{20}S_4$ $(M+H)^+$ 1736.2615, found 1736.2603.

*Synthesis of Isobacteriochlorin (**3**) and Bacteriochlorin (**4**).* These compounds are made using modifications of the previously reported procedure (*49*) and scaled up. A toluene (20 mL) solution of $TPPF_{20}$ (100 mg, 0.1 mmol), *N*-methylglycine (30 mg, 1 mmol), and paraformaldehyde (20 mg, 0.22 mmol) was heated at reflux for ca. 12 h under a nitrogen atmosphere. Further portions of *N*-methylglycine (30 mg) and

paraformaldehyde (20 mg) were again added, and the resulting mixture was refluxed for a total of 24 h (2 × 12 h). The compounds were separated by flash chromatography (silica gel) using hexane/CH_2Cl_2 (50:50 v/v) to elute the negligible amount of unreacted porphyrin **1**, followed by CH_2Cl_2 to get the chlorin **2** (45 mg, 42%) and then CH_2Cl_2/acetone (95:5) to get the isobacteriochlorin **3** (40 mg, 34%). However, we found that a small amount (ca. 10−15%) of the bacteriochlorin consistently elutes with the isobacteriochlorin under these conditions. Thus, compounds **2**, **3**, and **4** were separated using a petroleum ether/ethyl acetate gradient on a flash silica gel column. From 100 mg $TPPF_{20}$ (102.6 μmol) is obtained 70 mg of the chlorin compound **2** (67.89 μmol, 66% yield), 15 mg of the anti isobacteriochlorin compound **3** (13.77 μmol, 13% yield), and 5 mg of both the syn and anti bacteriochlorin compound **4** (4.6 μmol, 5% yield). The diastereomeric anti form of compound **3** is preferentially formed; conversely, the syn form of compound **4** is the major product (3:2 syn/anti), and the NMR, HRMS, and UV−visible spectra for **3** and **4** were consistent with the previous report (*49*).

*Synthesis of Protected Thioglycosylated Isobacteriochlorin, IGlcAc$_4$ (**3a**).* To a solution of isobacteriochlorin **3** (25 mg, 23 μmol) and 2,3,4,6-tetra-*O*-acetyl-glucosylthioacetate (40 mg, 103 μmol, 4.5 equiv) in DMF (2.5 mL), diethyl amine (0.5 mL) was added. The reaction mixture was stirred at room temperature for 4 h. The reaction mixture was precipitated with methanol/H_2O and the solid filtered through a short column of Celite and washed with water. The crude mixture was recovered in CH_2Cl_2 and purified by flash chromatography (silica gel) using a mixture of ethyl acetate/hexanes (3:1) as eluent. Isobacteriochlorin **3a** (49 mg, 86%) was obtained after crystallization in CH_2Cl_2/hexanes, as a pink powder. Because the *N*-methyl-pyrrolidine points to opposite faces of the isobacteriochlorin and of the stereo centers on the sugars, **3a** is made as a mixture of two sets of diastereomers on the four β-pyrrole positions bearing the *N*-methyl-pyrrolidine moieties. These are seen in some of the resonances in the ^{1}H NMR and especially the complexity of the phenyl region of the ^{13}C NMR, which shows the coupling to ^{19}F and the multiplicity due to the adjacent pair of diastereomers. mp > 250 °C. ^{19}F NMR (DMSO-d_6): δ −128.46 to −128.35, −128.81 to −128.70 (2m, 2F, Ar-*m*-F), −130.11 to −129.88, −130.45 to −130.35, −130.91 to −130.81 and −131.62 to −131.41 (4m, 6F, Ar-*m*-F), −136.79 to −136.64, −137.35 to −137.17, −139.42 to −139.23 and −140.04 to −139.94 (4m, 8F, Ar-*o*-F). ^{1}H NMR ($CDCl_3$): δ 7.64, 7.63, 7.22, 7.17 (4d, j = 5 Hz, 4H, pyrrolic β-H), 5.03−5.32 (m, 16H, Glc-H), 4.45−4.50 and 4.16−4.25 (2m, 14H, 4H β-H [C (sp^3)], 2H NH and 8H Glc-H), 3.83(d, j = 5 Hz, 4H, Glc-H), 2.70 and 2.88 (2t, j = 8.2 Hz, 4H, pyrrolidine-H), 2.06−2.31 (m, 58H, 4H pyrrolidine-H, 6H NCH_3, 48H, acetyl-H). ^{13}C NMR ($CDCl_3$): δ 20.6 ($\underline{C}H_3CO_2$), 41.0 (NCH_3), 47.8 and 51.7 (C2, C3, C7, and C8), 61.4, 61.8, 62.5 (CH_2 and Glc), 68.0, 70.2, 70.5, 73.81, 73.83, 76.3, 84.5 and 84.6 (Glc), 92.2, 98.2, 111.0, 111.1, 111.3, 113.6, 121.4, 121.5, 121.6, 128.5, 128.6, 144.4−148.7 (C_6F_4), 169.37, 169.38, 169.41, 170.16 and 170.62 ($CH_3\underline{C}O_2$). HRMS calcd. for $C_{106}H_{100}F_{16}N_6O_{36}S_4$ $(M)^{+\bullet}$ 2464.4806, found 2464.4700.

*Synthesis of Thioglycosylated Isobacteriochlorin, IGlc$_4$ (**3b**).* Isobacteriochlorin **3a** (30 mg, 12.1 μmol) was dissolved in methanol/CH_2Cl_2 (3:1, 4 mL) and treated with sodium methoxide (0.5 M solution in methanol, 1 mL). The reaction mixture was stirred at room temperature for 1 h and then neutralized by an aqueous citric acid solution. The mixture was filtered through Waters Sep-Pak C_{18} 35 cm^3 reverse-phase prep column and washed with water. The deprotected isobacteriochlorin **3b** was eluted with methanol and purified by flash chromatography (silica gel) using a mixture of ethyl acetate/methanol (3:2) as eluent. Isobacteriochlorin **3b** (19 mg, 88%) was obtained after crystallization in methanol/CH_2Cl_2 as a pink powder. **3b** is likewise a mixture of two sets of diastereomers. These are not resolved in the ^{1}H NMR, but are observed especially in the complexity of the phenyl region of the ^{13}C NMR, which shows the coupling to ^{19}F and the multiplicity due to the adjacent pair of diastereomers. mp > 250 °C. ^{19}F NMR (DMSO-d_6): δ −131.31 to −131.01, −132.98 to −132.25 and −133.68 to −133.43 (3m, 8F, Ar-*m*-F), −138.2 to −137.59, −140.13 to −140.04, −140.37 to −140.31 and −140.89 to −140.79 (4m, 8F, Ar-*o*-F). ^{1}H NMR (DMSO-d_6): δ 7.78 and 7.30 (2s, 4H, pyrrolic β-H), 5.67 (m, 4H, Glc-H), 5.21−5.24, 5.02−5.06 and 4.91−4.95 (3m, 12H, Glc-H), 4.40−4.44 and 4.05−4.13 (2m, 12H, 4H β-H [C (sp^3)], 2H NH, 8H Glc-H), 3.16−3.26 (m, 20H), Glc-H), 2.70, 2.57, 2.19 and 2.18 (4bs, 8H, pyrrolidine-H), 2.01 (s, 6H, NCH_3). ^{13}C NMR (DMSO-d_6/methanol-d_4): δ 40.6 (NCH_3), 47.7, 49.06 (C2, C3, C7, and C8), 61.5, 61.6, 61.7, 62.5, 70.48, 70.52, 75.0, 75.1, 78.44, 78.46, 78.48, 84.8, 85.0 (CH_2 and Glc), 92.2, 97.8 113.2, 113.3, 113.36, 113.38, 113.61, 119.0, 119.2, 146.0−148.6 (C_6F_4). HRMS calcd. for $C_{74}H_{69}F_{16}N_6O_{20}S_4$ $(M+H)^+$ 1793.3194, found 1793.3197.

*Synthesis of Protected Thioglycosylated Bacteriochlorin, BGlcAc$_4$ (**4a**).* To a solution of bacteriochlorin **4** (7 mg, 6.4 μmol) and 2,3,4,6-tetra-*O*-acetyl-glucosylthioacetate (12 mg, 29 μmol, 4.5 equiv) in DMF (0.5 mL), diethyl amine (0.1 mL) was added. The reaction mixture was stirred at room temperature for 4 h. Then, the reaction mixture was precipitated with methanol/H_2O, and the solid was filtered through a short column of Celite and washed with water. The crude mixture was recovered in CH_2Cl_2 and purified by flash chromatography (silica gel) using a mixture of ethyl acetate/hexanes (3:1) as eluent. Bacteriochlorin **4a** (13 mg, 86%) was obtained after crystallization in CH_2Cl_2/hexanes, as a green powder. Because of the stereo centers on the sugars, **4a** is made as a mixture of two sets of diastereomers. mp > 250 °C. ^{19}F NMR ($CDCl_3$): δ −129.05 to −128.15 (4m, 8F, Ar-*m*-F), −132.80 to −132.40 (m, 4F, Ar-*o*-F), −134.95 to −134.45 (m, 4F, Ar-*o*-F). ^{1}H NMR ($CDCl_3$): δ 8.30 (m, 4H, pyrrolic β-H), 5.12−5.23 (m, 20H, 16H Glc-H, 4H, β-H [C (sp^3)]), 4.15−4.30 (m, 8H Glc-H), 3.88 (m, 4H, Glc-H), 3.05−3.10 (m, 4H, pyrrolidine-H), 2.45−2.46 (m, 4H pyrrolidine-H), 2.06−2.31 (m, 54H, 6H NCH_3, 48H, 48H, acetyl-H), −1.75 (s, 2H, NH). ^{13}C NMR ($CDCl_3$): δ 20.6 (CH_3CO_2), 41.2 (NCH_3), 52.4 and 52.5 (C2, C3, C7, and C8), 61.7, 61.8 (CH_2 and Glc), 68.0, 70.6, 73.88, 76.70, 77.0, 77.3, 84.6 and 84.7 (Glc), 92.2, 99.7, 107.7, 111.4, 111.5, 115.5, 115.6, 122.6, 122.7, 136.0, 136.1, 144.4−148.7 (C_6F_4), 164.0, 169.38, 169.40, 170.19, and 170.64 (CH_3CO_2). HRMS calcd. for $C_{106}H_{100}F_{16}N_6O_{36}S_4$ $(M)^{+\bullet}$ 2464.4806, found 2464.4813.

*Synthesis of Thioglycosylated Bacteriochlorin, BGlc$_4$ (**4b**).* Bacteriochlorin **4a** (10 mg, 4.0 μmol) was dissolved in methanol/CH_2Cl_2 (3:1, 1.5 mL) and treated with sodium methoxide (0.5 M solution in methanol, 0.2 mL). The reaction mixture was stirred at room temperature for 1 h and then neutralized by an aqueous citric acid solution. The mixture is filtered through Waters Sep-Pak C_{18} 35 cm^3 reverse-phase prep column and washed with water. Though **4** has a plane of symmetry, because of the chiral centers on the sugars on **4a** and **4b**, these are prepared as a set of two diastereomers. The deprotected bacteriochlorin **4b** was eluted with methanol and purified by flash chromatography (silica gel) using a mixture of ethyl acetate/methanol (3:2) as eluent. Bacteriochlorin **4b** (6.5 mg, 88%) was obtained after crystallization in methanol/CH_2Cl_2, as a green powder. mp > 250 °C. ^{19}F NMR (MeOD): δ −134.0 to −132.5 (4m, 8F, Ar-*m*-F), −137.2 to −136.0 (m, 4F, Ar-*o*-F), −140.0 to −139.0 (m, 4F, Ar-*o*-F). ^{1}H NMR (MeOD): δ 8.42 (bs, 4H, pyrrolic β-H), 5.30−5.45 (m, 4H, Glc-H), 5.05−5.14 (m, 4H, β-H [C (sp^3)]), 3.73−3.74 and 3.63−3.65 (2m, 8H,

Glc-H), 3.49−3.54 and 3.41−3.43 (2m, 16H, 8H, and 8H Glc-H), 3.15−3.18 (m, 4H, pyrrolidine-H), 2.79−2.82 (m, 4H, pyrrolidine-H), 2.28 (s, 6H, NCH_3). ^{13}C NMR (MeOD): δ 39.8 (NCH_3), 51.8, 51.9 (C2, C3, C7, and C8), 61.6, 70.5, 74.57, 74.59, 78.3, 81.36, 81.37, 84.9, 85.12 (CH_2 and Glc), 99.91, 99.94, 100.0, 103.9, 113.32, 113.34, 113.45, 113.50, 120.86, 121.0, 136.2, 136.3, 136.4, 146.0−148.6 (C_6F_4). HRMS calcd. for $C_{74}H_{69}F_{16}N_6O_{20}S_4$ $(M+H)^+$ 1793.3194, found 1793.3179.

UV−visible, Fluorescence Spectroscopy, and Quantum Yield Calculations. UV−visible and fluorescence measurements were performed on dilute solutions, typically ~2 μM, of compounds in ethanol, phosphate buffered saline (PBS), and ethyl acetate. The UV−visible spectra were obtained from 330 to 800 nm using 1 cm quartz cuvettes. For steady-state fluorescence spectroscopy, samples were excited at 509 nm for ethyl acetate and 512 nm for PBS and ethanol where absorbencies are ≤0.1. For emission spectra, both the excitation and detection monochromators had a band-pass of 1 nm. The corrected emission (for instrument response) and absorption spectra were used to calculate the quantum yield. Fluorescence quantum yields were determined for chlorin, isobacteriochlorin, and bacteriochlorin solutions relative to TPP in toluene, which has a fluorescence quantum yield of 0.11 (*57, 58*). The quantum yields were measured indirectly using TPP; thus, these values may have some systematic error. All experiments were carried out on the same day, using identical concentrations to minimize any experimental errors. These three glycosylated conjugates are quite stable toward photobleaching. When ethanolic solution of $IGlc_4$ is exposed to sunlight with a power of ca. 40−80 W/m^2 for ca 2 h, we found only 10.5% of the compound decomposed (Supporting Information).

Quantum Yield of Singlet Oxygen Production (Φ_Δ). Φ_Δ values were determined on a relative basis by using *meso*-tetrakis(4-sulfonatophenyl)porphine dihydrochloride (TSPP) as a reference sensitizer ($\Phi_{\Delta,TSPP} = 0.7$ in methanol) (*56*). A time-resolved Nd:YAG laser (Polaris II, Electro Scientific Industries, Inc.) equipped with low-temperature cooled Ge detector (Applied Detector Corporation) was employed as an excitation source at 532 nm. All of the experiments were carried out in deuterium methanol-d_1. The absorbances from samples and TSPP at 532 nm were controlled between 0.1 and 0.5. $^1O_2$ luminescence was monitored as a function of sensitizer absorbance. Slopes were analyzed from a plot of $^1O_2$ intensity via absorbance. Φ_Δ can be calculated according to following equation:

$$\Phi_{\Delta,\text{sample}}/\Phi_{\Delta,\text{reference}} = \text{slope}_{\text{sample}}/\text{slope}_{\text{reference}}$$

Cell Culture. 3T3 K:MOLV NIH cells maintained in DMEM, 10% BCS, 1% antimycotic at 37 °C and in 5% CO_2 atmosphere were plated onto coverslips in cell culture dishes. $PGlc_4$, $CGlc_4$, and $IGlc_4$ dissolved in methanol were added to the cell cultures to a final concentration of 1 or 2.5 μM such that there was never more than 0.5% methanol in the solution. After 20 h incubation, cells were washed with PBS 3−5 times and fixed in 4% paraformaldehyde solution for 10 min at room temperature. The cells were then washed with PBS 3 times. The cells were visualized using a Nikon Optiphot 2 fluorescence microscope. Images were captured as JPEG files at 10× magnification, with a 505−565 nm excitation band-pass filter and a 565−685 nm emission band-pass filter. For each set of experiments, cells were cultured and the fluorescence images were taken under identical culture and microscopic conditions. For quantitative studies, the image intensities of the cells in the fluorescence micrographs were calculated by FLim program available at http://nathan.instras.com/projects/FLim/index.html.

Confocal Microscopy. Cells were plated onto coverslips in cell culture dishes. $BGlc_4$ dissolved in DMSO was added to the cultures to a final concentration of 10 μM (DMSO concentrations were <0.2%). After incubation for 24 h, the cells were rinsed three times with PBS and incubated with a 4% paraformaldehyde solution for 15 min at 37 °C under cell growth conditions. Cells were then washed three times with PBS, mounted in Dako fluorescence mounting medium, and visualized using a Zeiss LSM510 laser scanning confocal microscope where images were captured with excitation at 514 nm, emission used a 710−750 nm band-pass filter.

RESULTS AND DISCUSSION

The reduction of $TPPF_{20}$ is carried out by modifications of a reported 1,3-dipolar cycloaddition reaction of an azomethine ylide with $TPPF_{20}$, **1**, to produce chlorin **2**, isobacteriochlorin **3**, and bacteriochlorin **4** (Scheme 2) (*48, 49, 51*). The reaction is scaled up by 5-fold, and the chlorin, bacteriochlorin, and isobacteriochlorin products were separated by column chromatography using a petroleum ether/ethyl acetate gradient as eluent. When compound **3** is the target, the products are formed in yields of ca. 66% for **2**, 13% yield of the anti isomer of **3**, and 5% yields for the syn and anti isomers of the bacteriochlorin **4**. These yields are somewhat different from those reported, and reflect the yield of the isobacteriochlorin to the bacteriochlorin as ca. 5:1 rather than a few percent of the latter.

The mechanism of these dipolar additions has been discussed (*51*). Interestingly, chiral HPLC assays and CD spectra indicate a trace quantity of what is likely the product of a nonconcerted addition reaction in the crude reaction mixture in the synthesis of the chlorin. This may arise because of the stability of an intermediate conferred by the macrocycle (*59, 60*), but we did not pursue this. Statistically, the second dipolar addition reaction should prefer the adjacent pyrrole 2:1 over the opposite pyrrole, but IF_{20} is formed at 3:1. As with previous reports, for IF_{20} the anti structure (Scheme 2) forms predominantly by ca. 7-fold (*48, 49*), and our preliminary dynamics calculations indicate steric crowding between the *N*-methyl-pyrrolidine methylenes, and adjacent fluorophenyls result in distortion of the macrocycle and partial blocking of the syn face. In the case of the BF_{20}, the syn isomer is the major product. The dipolar addition mechanism in terms of MO calculations was discussed (*51*).

The principal goal was to obtain the four compounds in one step and in sufficient quantity for the next reactions. NMR and mass spectrometry are consistent with the previous report and attest to the purity of these porphyrinoid-F_{20} intermediates. The nucleophilic substitution of the thioglucose at the para position of the perfluorophenyl substituents of these porphyrinoids is a modification of that previously reported (*33*). Specifically, 4.5 equiv of 1-thioacetate-2,3,4,6-tetra-*O*-acetyl-β-D-glucopyranose, a greater quantity of diethylamine (DEA), in 1 h reactions yields $PGlcAc_4$ **1a**. Thus, **2a** ($CGlcAc_4$), **3a** ($IGlcAc_4$), and **4a** ($BGlcAc_4$) are obtained from **2**, **3**, and **4**, respectively (Scheme 2). More than four thiosugars can be added with greater equivalents and longer reaction times. Flash chromatography yields the protected glycosylated derivatives as the mixture of diastereomers in ca. 85% yields. The carbohydrate protection groups were removed by treating **1a**, **2a**, **3a**, and **4a** with sodium methoxide in dry methanol to obtain the glycoporphyrinoids **1b**, **2b**, **3b**, and **4b** in ca. 95−98% yield (Scheme 2) (Supporting Information).

Since the *N*-methyl-pyrrolidine points toward one face of the macrocycle, addition of moieties with chiral centers such as the sugars to chlorin **2** results in diastereomers at the *N*-methylpyrrolidine β-carbons for **2a** and **2b**, even though **2** has a plane of symmetry. Thus, **2a** and **2b** are 2R,3S diastereomers, which was not previously recognized. As pointed out in the synthesis (*51*), there is a set of enantiomers at the β-carbons for the anti conformer of **3**; thus, the addition of the sugars further

Scheme 3. $CGlc_4$ Diastereomers (see Supporting Information)

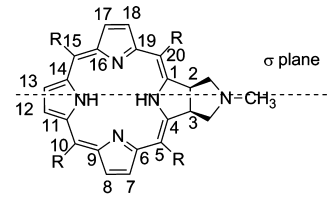

(2*R*,3*S*) - meso when R is achiral

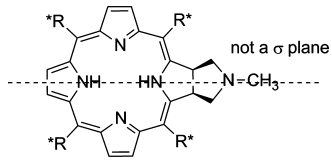

(2*R*,3*S*) - optically active
diastereomer when R* is chiral

differentiates these in **3a** and **3b** into diastereomers 2R,3S,7S,8R and 2S,3R,7R,8S. Both the syn and anti forms of bacteriochlorin **4** have a plane of symmetry, but addition of the sugars results in a set of diastereomers, 2R,3S,12S,13R and 2S,3R,12R,13S (Scheme 3).

The structures of all porphyrinoids were confirmed by NMR, UV−visible, and mass spectrometry and HRMS analysis. The ^{1}H NMR spectra of **2a**, **3a**, and **4a** show the porphyrinoid core pyrrole β protons near 8.9 ppm and the pyrrole NH protons near −2 ppm. The ^{1}H NMR spectra of all three compounds show resonance at 2.1 and 2.3 ppm, due to the acetyl protons, and the resonances of the other protons of the carbohydrate unit appear between 4 and 6 ppm. The resonances of the anomeric protons appear as doublets at 5.03 ppm to 5.40 ppm. The N-methyl groups are observed in the 2.22 ppm for **2a** and are obscured by the acetyl groups in **3a** and **4a**. While the diastereomers are observed for some resonances for the protected derivatives, they are not well-resolved for **2b**, **3b,** and **4b**.

The ^{19}F NMR spectra confirm the substitution of the para-fluorine atom by the sugar unit, showing the disappearance of the resonances due to the para-fluorine atoms in **2**, **3**, and **4** at −150 ppm. An important diagnostic is the signal due to the meta-fluorine atom shift from −160 ppm in **2**, **3**, and **4** to −130 ppm for **2a**, **3a**, and **4a**. The ortho-fluorine atom resonances remain near −140 ppm. The ^{19}F NMR spectra do not exhibit marked differences between **2a** and **2b**, **3a** and **3b**, or **4a** and **4b**, though these peaks are broadened due to the diastereomeric centers. The ^{13}C NMR clearly indicates the multiple resonances arising from the diastereomers, especially for the phenyl carbons, which remain coupled to the F-atoms, and are closest to the chiral centers of **2a**, **2b**, **3a**, **3b**, **4a**, and **4b**.

Considering the large dependence of the photophysical properties of polar chromophores on the solvent matrix and on other experimental parameters, it is important to develop a self-consistent set of data for accurate comparison of these properties and assessment of potential applications. Since the dye can partition into lipophilic, hydrophilic, or amphipathic cellular structures, we have assayed the photophysical properties in three different solvents. Thus, PBS at pH = 7.4, ethanol, and ethyl acetate solvents were used to probe the photophysical properties (the partition coefficients and photophysical properties are summarized in Tables 1 and 2). While the initial association with the cell is mediated by glucose receptors and the four glycosyl groups on the chromophore, some nonspecific partition into the membrane is also indicated. Because of the size of the molecules, uptake is unlikely to proceed by active or passive transport, but the high local concentration around the cell increases diffusion. Thus, uptake is also dependent on the relative hydrophobicity of the compounds (*61*). The octanol/water partition coefficient and R_f for the glycosylated compounds are listed in Table 1.

Table 1. Partition Coefficients

compound	octanol/water	R_f[a]
$PGlc_4$	43.9 (4.8)	0.6 (5.5)
$CGlc_4$	28.5 (3.13)	0.37 (3.4)
$IGlc_4$	9.1 (1)	0.11 (1)
$BGlc_4$	12.7 (1.4)	0.13 (1.2)

[a] Normalized values in parentheses; see Experimental Section.

The electronic spectra of **2**, **3**, and **4** and the glycosylated derivatives are significantly different from the $TPPF_{20}$. The lowest-energy Q-band of chlorin, $CGlc_4$, in PBS buffer at 649 nm has about 25-fold greater intensity than corresponding Q-band of porphyrin $PGlc_4$ at 646 nm. For isobacteriochlorin, $IGlc_4$ in the same buffer, the lowest-energy Q-band at 645 nm is 5-fold more intense than the porphyrin at the same wavelength. For $BGlc_4$, the strong lowest-energy peak is located at 730 nm improving the absorption in the red region of the spectrum. The fluorescence emission spectra for the four glycosylated porphyrinoids are correspondingly different and have a strong solvent dependence (Table 2).

There are negligible Stokes shifts for $PGlc_4$, $CGlc_4$, and $BGlc_4$ in the three solvents, indicating minimal specific solvent−solute interactions with the macrocycle effecting vibrational processes (*62*). Notably, for the $IGlc_4$ in PBS, the strongest fluorescence band λ_{max} is at 606 nm with a weaker emission centered at 650 nm, while for $BGlc_4$, the peak is presented at 725 nm. Excitation spectra all indicate the presence of only the given compounds. The 0.17 and 0.36 fluorescence quantum yields for $CGlc_4$ and for $IGlc_4$ in PBS are 6 times and 12 times, respectively, that of the porphyrin analogue $PGlc_4$, while for $BGlc_4$ it is 0.03, similar to the $PGlc_4$. There is a small decrease in fluorescence quantum yield upon replacement of the para F atom by the thiocarbohydrate group due to both electronic and heavy atom effects. The greater fluorescence quantum yield of **2b** than m-THPC (*13*) or a water-soluble dimeso substituted chlorin (*10*) likely arises from the presence of the 16 F groups and relative energies of the molecular orbitals, and is consistent with the quantum yield of singlet oxygen generation by **2** (*63*). However, tetraarylporphyrins with a tripeptide (*64*) and other meso aryl chlorins (*65*) have similar photophysical properties to what we find. The sugars have little direct effect on the photophysics but modulate the amphipathicity and enable the observed solvent dependence.

The quantum yields of singlet oxygen formation for three of the compounds in methanol-d_1 are listed in Table 2. Since the porphyrin ring is the reactive site for $^1O_2$ production, the frequency of collisions that result in the formation of $^1O_2$ is related to the probability that an $^3O_2$ molecule makes physical contact with the chromophore in the excited, triplet state. The additional steric effect of the pyrrolidine-fused rings on $CGlc_4$ and $IGlc_4$ could result in reduced collision frequencies and a lower Φ_Δ compared to $PGlc_4$. It is reasonable to expect that internal conversion is somewhat consistent between the compounds, so the increased fluorescence quantum yield means a decrease in the amount of triplet formed. The Φ_Δ data dovetail with the observe fluorescence yields, but the Φ_Δ for $IGlc_4$ in methanol is more consistent with the PBS buffer data.

Because our previous studies with thioglycosylated porphyrin $PGlc_4$ indicated good uptake and photodynamic effects on several cancer cell lines, K:Molv NIH 3T3 mouse fibroblasts (Figure 2) and the MDA-MB-231 breast cancer cell line were used to evaluate the cellular uptake of the glycosylated

Table 2. Photophysical Properties of Glycosylated Porphyrinoid Derivatives

compound	solvent	UV−visible[a]	emission λ_{max}	Φ_F[b]	$^1O_2$ Φ_Δ
$TPPF_{20}$	DMSO	412, 504, 538, 580, 632	637, 702	--	
CF_{20}	DMSO[c]	408, 504, 536, 598, 652	656	--	
m-THPC	methanol[d]		653, 720	0.09	0.43
m-THPBC	methanol[d]		612, 653, 746	0.11	0.43
$PGlc_4$	ethanol	412, 505, 535, 586, 653	653, 702	0.05	0.85[f]
	PBS buffer	410, 510, --- 576, 646(1)[a]	646, 692	0.03	
	ethyl acetate	412, 507, 450, 583, 655	649, 701	0.05	
	DMSO[c]	415, 507, 539, 581, 636	640, 705	0.06	
$CGlc_4$	ethanol	408, 507, 534, 599, 653	653, 715	0.43	0.32[f]
	PBS buffer	409, 506, 533, 597, 649(25)[a]	649, 707	0.17	
	ethyl acetate	406, 504, 531, 597, 651	653, 712	0.39	
	DMSO[e]	412, 506, 537, 598, 652	652	--	0.28
$BGlc_4$	ethanol	353, 374, 505, 732	729	0.047	--
	PBS buffer	357, 508, 730	725	0.03	
	ethyl acetate	352, 379, 508, 730	730	0.055	
$IGlc_4$	ethanol	385, 513, 548, 588, 643	596, 646, 705	0.70	0.59[f]
	PBS buffer	385, 513, 548, 593, 645(5)[a]	606, 650, 711	0.36	
	ethyl acetate	384, 510, 548, 589, 653	596, 646, 700	0.60	

[a] Relative intensity of lowest-energy Q bands. [b] Fluorescence experiments done in air. [c] Taken from ref *55*. [d] m-THPC and the bacteriochlorin m-THPBC taken from ref *13*. [e] Taken from ref *54*. [f] Excited at 532 nm in methanol-d_1.

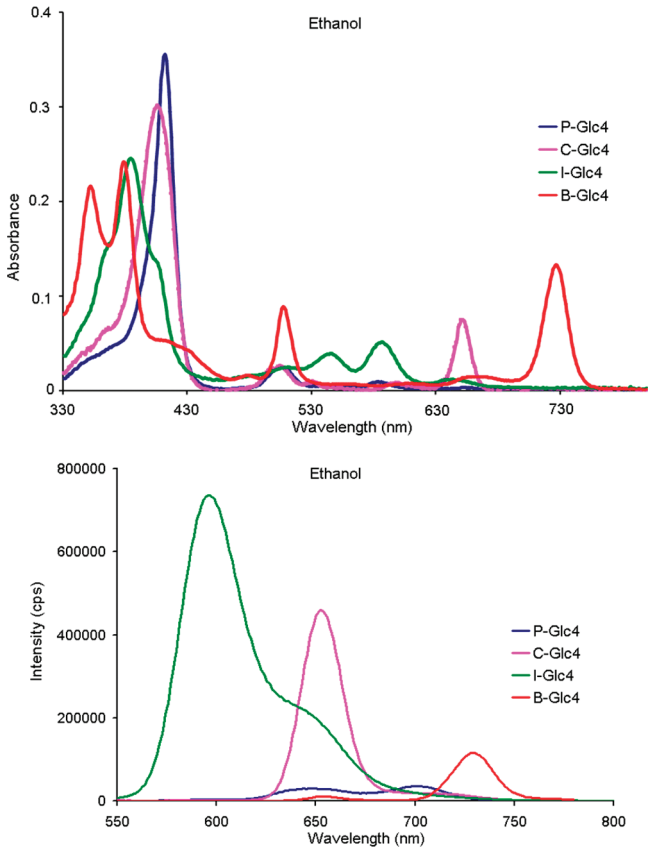

Figure 1. Top: UV−visible spectra of the compounds, 2 μM in ethanol. Bottom: emission spectra of the compounds in ethanol; excitation at 512 nm where the absorbance is ca. 0.05 for each compound.

derivatives. Our initial hypothesis was that the *N*-methylpyrrolidine moieties used to make and stabilize the chlorin, bacteriochlorin, and isobacteriochlorin (as well as the stereo centers at the β positions) would have minimal effect on cell uptake, because these are sandwiched between the glycosylated tetrafluorophenyl groups. K:Molv NIH 3T3 cells were incubated identically with 2.5 μM concentrations of $PGlc_4$, $CGlc_4$, and $IGlc_4$, rinsed with buffer, and the relative uptake was quantified by comparison of images taken by fluorescence microscopy under identical settings (*38*). Confocal microscopy using 10 μM $BGlc_4$ was used because the red absorption and emission are outside the range of our fluorescence microscope (Figure 3). The electronic spectra, fluorescence, and fluorescence microscopy studies all show that these compounds are robust to photobleaching. The remaining 16 F groups impart oxidative stability and further enhance the photonic properties.

At 2.5 μM, the relative integrated intensities for $PGlc_4$, $CGlc_4$, and $IGlc_4$ in the fluorescence micrographs of the K:Molv NIH 3T3 are 1:2:7, respectively (Figure 2). Taking into consideration both the partition coefficients and the fluorescence quantum yields, one would expect that the relative uptake of these compounds into the cells measured by fluorescence to be ca. 1:4:2 for the $PGlc_4$/$CGlc_4$/$IGlc_4$, respectively. The disparity may arise from differences in cell specificity or the degree of aggregation of the compounds in the PBS buffer and/or aggregation as the local concentration of the dyes around the cell increases (*17*). The propensity of aggregation inside the cell may also vary. Also, some diastereomers may be taken up preferentially over others. The mechanism of uptake and photodynamic effects in this and other cell lines will be reported elsewhere.

Though there may be differences in uptake among these compounds, we have shown that the $PGlc_4$ compound localizes in the endoplasmic reticulum because of the metabolic needs of this organelle (*43*). The significantly greater fluorescence quantum yield of the $IGlc_4$ system means that ca. 25 nM concentrations can be used to follow receptors and/or glycolysis processes in the cell (Figure 4). Thus, $IGlc_4$ is better suited for tagging and sensor applications. For PDT applications, sensitizers with strong red absorptions are generally considered better because these wavelengths penetrate deeper into tissue (*6, 7*). The optical cross section of $CGlc_4$ in the red region is significantly larger than the porphyrin or isobacteriochlorin analogues. Thus, if red light is used to activate the second-generation dye $CGlc_4$, the increased light absorptivity more than compensates the reduced triplet quantum yield. Given the very strong 730 nm absorption, the low fluorescence quantum yield, and the greater triplet quantum yield of $BGlc_4$, this may be the best photosensitizer for PDT of the compounds described herein. However, a more efficient synthesis and purification of the isomers and diastereomers needs to be developed for the bacteriochlorin compounds to be used. The detailed photophysics of these compounds, including in biological systems, will be the subject of future studies.

Though the fluorescence of $CGlc_4$ and $IGlc_4$ is greater than that of the parent porphyrin, there is still sufficient triplet formation to effect cell death via necrosis and/or apoptosis. This indicates that these compounds can be used as dual function

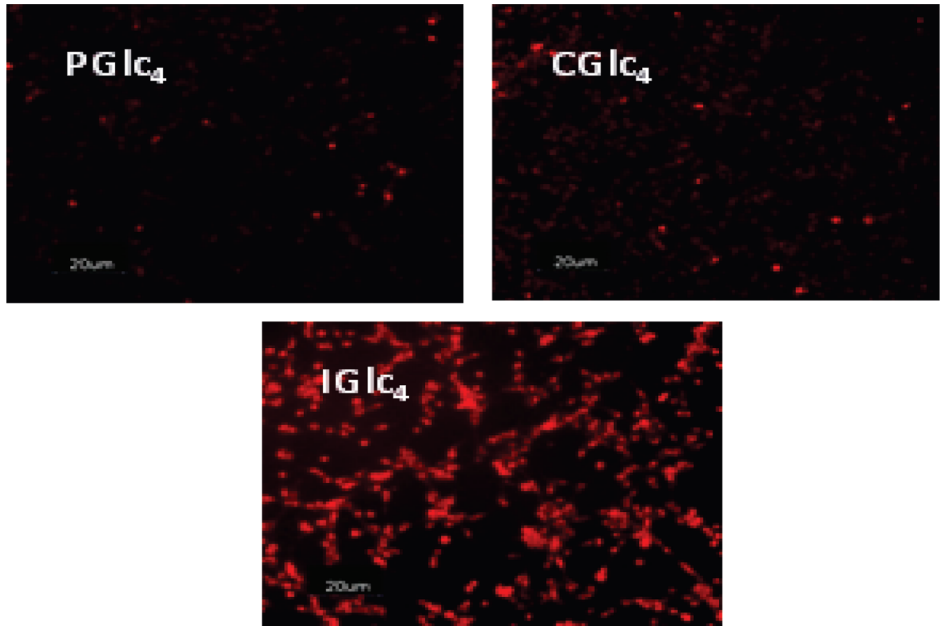

Figure 2. Fluorescence microscopy of K:Molv NIH 3T3 cells treated with 2.5 μM $PGlc_4$ (**1b**), $CGlc_4$ (**2b**), and $IGlc_4$ (**3b**). K:Molv NIH 3T3 cells were incubated for 20 h with porphyrinoids, followed by removal of unbound dye from the cell culture by repeated rinsing with PBS, and the cells were imaged under identical microscope settings and not enhanced; magnification 10×.

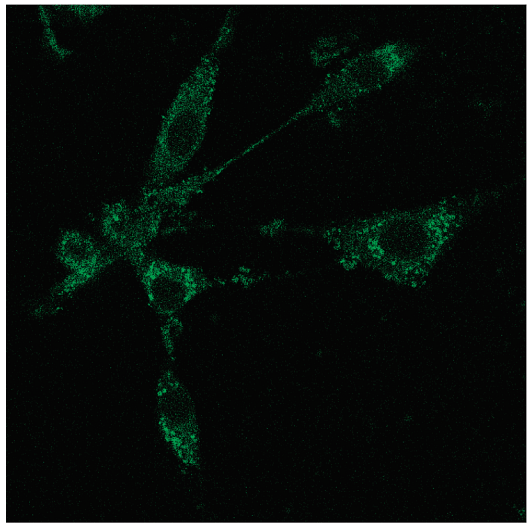

Figure 3. K:Molv NIH 3T3 cells were incubated with 10 μM $BGlc_4$ for 24 h, rinsed three times with PBS buffer, and fixed with 4% paraformaldehyde solution. Confocal microscope excitation at 514 nm, emission monitored with a 710−750 band-pass filter. No images are observed using a 610−650 nm emission band-pass filter, so fluorescence does not arise from the one of the other dye systems. The image is not enhanced; magnification is 60×.

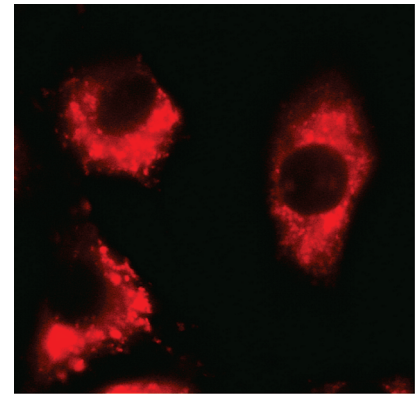

Figure 4. Fluorescence image of a MDA-MB-231 breast cancer cell treated with 25 nM $IGlc_4$ and rinsed three times with PBS buffer to remove unbound dye (see Supporting Information for comparisons to the other porphyrinoids).

agents that both locate and treat cancerous cells. To demonstrate PDT activity, $CGlc_4$ and $IGlc_4$ were tested under the same conditions as $PGlc_4$ (10 μM concentration and 10 min irradiation with white light from a 13 W fluorescent bulb). $CGlc_4$ and $IGlc_4$ induce cell death only after twice the light power is used (data not shown).

We have also made the chlorin via a gemdiol on one pyrrole unit of $TPPF_{20}$ and the corresponding tetraglycosylated derivative (*47, 66*), but the yield and stability are not as good as the those of the compounds described herein (Supporting Information). Similar to the parent $TPPF_{20}$, preliminary studies indicate the same high-yield substitution chemistry can yield an array of conjugates on these core platforms to target various tissues (*2, 34, 38*), cell types, and cellular structures (*67*).

In conclusion, these core platforms will enable rapid development of new multifunctional imaging, sensing, and therapeutic agents (*68*) for specific targets, and the ability to assess the effectiveness appended motifs in targeting. These platforms will also facilitate the development of effective probes for fundamental biochemical/biophysical studies (*44, 69*). Both $CGlc_4$ and $IGlc_4$ have significantly enhanced fluorescence quantum yields compared to $PGlc_4$, while the $BGlc_4$ derivative has a fluorescence quantum yield that is similar to the parent porphyrin. Thus, $IGlc_4$ has greatest potential use as fluorescent tags, diagnostics, or imaging agents. The intermediate fluorescence of the $CGlc_4$ system may well serve as a dual purpose agent for targeting, detecting, and treating diseased tissues. The $BGlc_4$ system has near-optimal properties as the PDT agent, but new synthetic strategies are needed to make these compounds.

ACKNOWLEDGMENT

Supported by National Institutes of Health (NIH) GM60654 to C.M.D.; KL2RR024997 for J.P.C.T. and UL1RR024996 for S.T. of the Clinical and Translational Science Center at Weill Cornell Medical College UL1-RR024996; and National Science

Foundation (NSF) CHE-0847997 to C.M.D. R.G. acknowledges support from NSF-PREM (DMR-0611539) and NIH-RCMI (2G12-RR-013459). Hunter College Chemistry infrastructure is supported by the NSF, NIH, including the RCMI program (G12-RR-03037), and the City University of New York.

Supporting Information Available: Additional spectroscopic data including ^{1}H NMR, ^{13}C NMR, ^{19}F NMR, and HRMS of all the protected and deprotected glycosylated porphyrinoids, UV−visible and fluorescence spectra in three different solvents: PBS, ethanol, and ethyl acetate, diastereomeric structures of CF_{20} and IF_{20}, CD spectra of CF_{20}, IF_{20}, and BF_{20} in chloroform, CD spectra of $CGlc_4$, $IGlc_4$, and $BGlc_4$ in methanol, cell uptake fluorescence images using MDA-MB-231 breast cancer cell line, singlet oxygen quantum yield data, and photobleaching experiment of $IGlc_4$ in sunlight. Spectroscopic characterization of the compounds and the substitution of a diol chlorin outlined. This material is available free of charge via the Internet at http://pubs.acs.org.

LITERATURE CITED

(1) Kadish, K., Smith, K. M., and Guilard, R. (2000, 2003) *The Porphyrin Handbook*, Vol. 1−20, Academic Press, New York.

(2) Drain, C. M., and Singh, S. (2010) Combinatorial libraries of porphyrins: Chemistry and applications, In *The Handbook of Porphyrin Science with Applications to Chemistry, Physics, Materials Science, Engineering, Biology and Medicine* (Kadish, K., Smith, K. M., and Guilard, R., Eds.) pp 485−537, World Scientific Publisher, Singapore.

(3) Smith, K. M. (1972) *Porphyrins and Metalloporphyrins*, Elsevier, Amsterdam.

(4) Dolphin, D. (1978) *The Porphyrins*, Academic Press, London.

(5) Sternberg, E. D., Dolphin, D., and Brückner, C. (1998) Porphyrin-based photosensitizers for use in photodynamic therapy. *Tetrahedron 54*, 4151–4202.

(6) Bonnett, R. (1995) Photosensitizers of the porphyrin the phthalocyanine series for phtodynamic therapy. *Chem. Soc. Rev. 24*, 19–33.

(7) Pandey, R. K. (2000) Recent advances in photodynamic therapy. *J. Porphyrins Phthalocyanines 4*, 368–373.

(8) Pandey, R. K., and Zheng, G. (2000) Porphyrins as photosensitizers in photodynamic therapy, In *The Porphyrin Handbook* (Kadish, K. M., Smith, K. M., and Guilard, R., Eds.) pp 157−230, Academic Press, London.

(9) Laville, I., Figueiredo, T., Loock, B., Pigaglio, S., Maillard, P., Grierson, D. S., Carrez, D., Croisy, A., and Blais, J. (2003) Synthesis, cellular internalization and photodynamic activity of glucoconjugated derivatives of tri and tetra(meta-hydroxyphenyl)chlorins. *Bioorg. Med. Chem. 11*, 1643–1652.

(10) Borbas, K. E., Chandrashaker, V., Muthiah, C., Kee, H. L., Holten, D., and Lindsey, J. S. (2008) Design, synthesis, and photophysical characterization of water-soluble chlorins. *J. Org. Chem. 73*, 3145–3158.

(11) Yihui, C., Guolin, L., and Ravindra, K. P. (2004) Synthesis of bacteriochlorins and their potential utility in photodynamic therapy (PDT). *Curr. Org. Chem. 8*, 1105–1134.

(12) Huang, Y.-Y., Mroz, P., Zhiyentayev, T., Sharma, S. K., Balasubramanian, T., Ruzi, C., Krayer, M., Fan, D., Borbas, K. E., Yang, E., Kee, H. L., Kirmaier, C., Diers, J. R., Bocian, D. F., Holten, D., Lindsey, J. S., and Hamblin, M. R. (2010) In vitro photodynamic therapy and quantitative structure-activity relationship studies with stable synthetic near-infrared-absorbing bacteriochlorin photosensitizers. *J. Med. Chem. 53*, 4018–4027.

(13) Bonnett, R., Charlesworth, P., Djelal, B. D., Foley, S., McGarvey, D. J., and Truscott, T. G. (1999) Photophysical properties of 5,10,15,20-tetrakis(*m*-hydroxyphenyl)-porphyrin (*m*-THPP), 5,10,15,20-tetrakis(*m*-hydroxyphenyl)chlorin (m-THPC) and 5,10,15,20-tetrakis(*m*-hydroxyphenyl)bacteriochlorin (m-THPBC): a comparative study. *J. Chem. Soc., Perkin Trans. 2*, 325–328.

(14) Nguyen, Q. T., Olson, E. S., Aguilera, T. A., Jiang, T., Scadeng, M., Ellies, L. G., and Tsien, R. Y. (2010) Surgery with molecular fluorescence imaging using activatable cell-penetrating peptides decreases residual cancer and improves survival. *Proc. Natl. Acad. Sci., U.S.A. 107*, 4317–4322.

(15) Mikata, Y., Onchi, Y., Tabata, K., Ogura, S.-i., Okura, I., Ono, H., and Yano, S. (1998) Sugar-dependent photocytotoxic property of tetra- and octa-glycoconjugated tetraphenylporphyrins. *Tetrahedron Lett. 39*, 4505–4508.

(16) Chen, X., and Drain, C. M. (2004) Photodynamic therapy using carbohydrate conjugated porphyrins. *Drug Des. Rev. 1*, 215–234.

(17) Csik, G., Balog, E., Voszka, I., Tölgyesi, F., Oulmi, D., Maillard, P., and Momenteau, M. (1998) Glycosylated derivatives of tetraphenyl porphyrin: photophysical characterization, self-aggregation and membrane binding. *J. Photochem. Photobiol., B 44*, 216–224.

(18) Obata, M., Hirohara, S., Sharyo, K., Alitomo, H., Kajiwara, K., Ogata, S.-i., Tanihara, M., Ohtsuki, C., and Yano, S. (2007) Sugar-dependent photodynamic effect of glycoconjugated porphyrins: A study on photocytotoxicity, photophysical properties and binding behavior to bovine serum albumin (BSA). *Biochim. Biophys. Acta 1770*, 1204–1211.

(19) Gomes, A. T. P. C., Leão, R. A. C., Silva, F. C. d., Neves, M. G. P. M. S., Faustino, M. A. F., Tomé, A. C., Silva, A. M. S., Pinheiro, S., Souza, M. C. B. V. d., Ferreira, V. F., and Cavaleiro, J. A. S. (2009) Synthesis of new glycoporphyrin derivatives through carbohydrate-substituted α-diazoacetates. *J. Porphyrins Phthalocyanines 13*, 247–255.

(20) Hirohara, S., Obata, M., Ogata, S.-i., Ohtsuki, C., Higashida, S., Ogura, S.-i., Okura, I., Takenaka, M., Ono, H., Sugai, Y., Mikata, Y., Tanihara, M., and Yano, S. (2005) Cellular uptake and photocytotoxicity of glycoconjugated chlorins in HeLa cells. *J. Photochem. Photobiol., B 78*, 7–15.

(21) Hirohara, S., Obata, M., Alitomo, H., Sharyo, K., Ogata, S.-i., Ohtsuki, C., Yano, S., Ando, T., and Tanihara, M. (2008) Structure-photodynamic effect relationships of 24 glycoconjugated photosensitizers in HeLa cells. *Biol. Pharm. Bull. 31*, 2265–2272.

(22) Maillard, P., Loock, B., Grierson, D. S., Laville, I., Blais, J., Doz, F., Desjardins, L., Carrez, D., Guerquin-Kern, J. L., and Croisy, A. (2007) In vitro phototoxicity of glycoconjugated porphyrins and chlorins in colorectal adenocarcinoma (HT29) and retinoblastoma (Y79) cell lines. *Photodiag. Photodyn. Ther. 4*, 261–268.

(23) Zorlu, Y., Ermeydan, M. A., Dumoulin, F., Ahsen, V., Savoie, H., and Boyle, R. W. (2009) Glycerol and galactose substituted zinc phthalocyanines. Synthesis and photodynamic activity. *Photochem. Photobiol. Sci. 8*, 312–318.

(24) Okada, M., Kishibe, Y., Ide, K., Takahashi, T., and Hasegawa, T. (2009) Convenient approach to access octa-glycosylated porphyrins via "click chemistry". *Int. J. Carbohydr. Chem.* 305276.

(25) Amessou, M., Carrez, D., Patin, D., Sarr, M., Grierson, D. S., Croisy, A., Tedesco, A. C., Maillard, P., and Johannes, L. (2008) Retrograde delivery of photosensitizer (TPPp-O-beta-GluOH)$_3$ selectively potentiates its photodynamic activity. *Bioconjugate Chem. 19*, 532–538.

(26) Iqbal, Z., Hanack, M., and Ziegler, T. (2009) Synthesis of an octasubstituted galactose zinc(II) phthalocyanine. *Tetrahedron Lett. 50*, 873–875.

(27) Soares, A. R. M., Tomé, J. P. C., Neves, M. G. P. M. S., Tomé, A. C., Cavaleiro, J. A. S., and Torres, T. (2009) Synthesis of water-soluble phthalocyanines bearing four or eight D-galactose units. *Carbohydr. Res. 344*, 507–510.

(28) Hirohara, S., Nishida, M., Sharyo, K., Obata, M., Ando, T., and Tanihara, M. (2010) Synthesis, photophysical properties and photocytotoxicity of mono-, di-, tri- and tetra-glucosylated fluorophenylporphyrins. *Biorg. Med. Chem. 18*, 1526–1535.

(29) Elmer, S. L., Man, S., and Zimmerman, S. C. (2008) (2008) Synthesis of polyglycerol, porphyrin-cored dendrimers using click chemistry. *Eur. J. Org. Chem.* 3845–3851.

(30) Grin, M. A., Lonin, I. S., Makarov, A. I., Lakhina, A. A., Toukach, F. V., Kachala, V. V., Orlova, A. V., and Mironov, A. F. (2008) Synthesis of chlorin-carbohydrate conjugates by 'click chemistry'. *Mendeleev Commun. 18*, 135–137.

(31) Mikata, Y., Sawaguchi, T., Kakuchi, T., Gottschaldt, M., Schubert, U. S., Ohi, H., and Yano, S. (2010) (2010) Control of the Aggregation properties of tris(maltohexaose)-linked porphyrins with an alkyl chain. *Eur. J. Org. Chem.* 663–671.

(32) Chen, X., Hui, L., Foster, D. A., and Drain, C. M. (2004) Efficient synthesis and photodynamic activity of porphyrin-saccharide conjugates: targeting and incapacitating cancer cells. *Biochemistry 43*, 10918–10929.

(33) Pasetto, P., Chen, X., Drain, C. M., and Franck, R. W. (2001) Synthesis of hydrolytically stable porphyrin C- and S-glycoconjugates in high yields. *Chem. Commun.* 81–82.

(34) Drain, C. M., Singh, S., Samaroo, D., Thompson, S., Vinodu, M., and Tomé, J. P. C. (2009) New porphyrin glyco-conjugates. *Proc. Soc. Photo Opt. Instrum. Eng.* 7380.

(35) Drain, C. M., Varotto, A., and Radivojevic, I. (2009) Self-organized porphyrinic materials. *Chem. Rev. 109*, 1630–1658.

(36) Varotto, A., Todaro, L., Vinodu, M., Koehne, J., Liu, G.-y., and Drain, C. M. (2008) Self-organization of a new fluorous porphyrin and C_{60} films on indium-tin-oxide electrode. *Chem. Commun.* 4921–4923.

(37) Samaroo, D., Soll, C. E., Todaro, L. J., and Drain, C. M. (2006) Efficient microwave-assisted synthesis of amine substituted pentafluorophenylporphyrin. *Org. Lett. 8*, 4985–4988.

(38) Samaroo, D., Vinodu, M., Chen, X., and Drain, C. M. (2007) meso-tetra(pentafluorophenyl)porphyrin as an efficient platform for combinatorial synthesis and the selection of new photodynamic therapeutics using a cancer cell line. *J. Comb. Chem. 9*, 998–1011.

(39) Shaw, S. J., Edwards, C., and Boyle, R. W. (1999) Regioselective synthesis of multifunctionalizd porphyrins - coupling of mono-(pentafluorophenyl)porphyrins to electrophiles. *Tetrahedron Lett. 40*, 7585–7586.

(40) Shaw, S. J., Elgie, K. J., Edwards, C., and Boyle, R. W. (1999) Mono-(pentafluorophenyl)porphyrins - Useful intermediates in the regioselective synthesis of multifunctionalised porphyrins. *Tetrahedron Lett. 40*, 1595–1596.

(41) Traylor, T. G., Byun, Y. S., Traylor, P. S., Battioni, P., and Mansuy, D. (1991) Polymeric polyhalogenated metalloporphyrin catalysts for hydroxylation of alkanes and epoxidation of alkenes. *J. Am. Chem. Soc. 113*, 7821–7823.

(42) Králová, J., Bříza, T., Moserová, I., Dolenský, B., Vašek, P., Poučková, P., Kejík, Z., Kaplánek, R., Martásek, P., Dvořák, M., and Král, V. (2008) Glycol porphyrin derivatives as potent photodynamic inducers of apoptosis in tumor cells. *J. Med. Chem. 51*, 5964–5973.

(43) Thompson, S., Chen, X., Hui, L., Toschi, A., Foster, D. A., and Drain, C. M. (2008) Low concentrations of a non-hydrolysable tetra-S-glycosylated porphyrin and low light induces apoptosis in human breast cancer cells via stress of the endoplasmic reticulum. *Photochem. Photobiol. Sci. 7*, 1415–1421.

(44) Plaetzer, K., Kiesslich, T., Oberdanner, C. B., and Krammer, B. (2005) Apoptosis following photodynamic tumor therapy: Induction, mechanisms and detection. *Curr. Pharm. Des. 11*, 1151–1165.

(45) Pandey, S. K., Gryshuk, A. L., Graham, A., Ohkubo, K., Fukuzumi, S., Dobhal, M. P., Zheng, G., Ou, Z., Zhan, R., Kadish, K. M., Oseroff, A., Ramaprasad, S., and Pandey, R. K. (2003) Fluorinated photosensitizers: synthesis, photophysical, electrochemical, intracellular localization, in vitro photosensitizing efficacy and determination of tumor-uptake by 19F in vivo NMR spectroscopy. *Tetrahedron 59*, 10059–10073.

(46) Mauzerall, D. C. (1998) Evolution of porphyrins. *Clin. Dermatol. 6*, 195–201.

(47) Brückner, C., McCarthy, J. R., Daniell, H. W., Pendon, Z. D., Ilagan, R. P., Francis, T. M., Ren, L., Birge, R. R., and Frank, H. A. (2003) A spectroscopic and computational study of the singlet and triplet excited states of synthetic [beta]-functionalized chlorins. *Chem. Phys. 294*, 285–303.

(48) Silva, A. M. G., Tomé, A. C., Neves, M. G. P. M. S., Silva, A. M. S., and Cavaleiro, J. A. S. (1999) meso-Tetraarylporphyrins as dipolarophiles in 1,3-dipolar cycloaddition reactions. *Chem. Commun.* 1767–1768.

(49) Silva, A. M. G., Tome', A. C., Neves, M. G. P. M. S., Silva, A. M. S., and Cavaleiro, J. A. S. (2005) 1,3-Dipolar cycloaddition reactions of porphyrins with azomethine ylides. *J. Org. Chem. 70*, 2306–2314.

(50) Cavaleiro, J. A. S., Tomé, A. C., and Neves, M. G. P. M. S. (2010) meso-Tetraarylporphyrin derivatives: New synthetic methodologies, In *The Handbook of Porphyrin Science with Applications to Chemistry, Physics, Materials Science, Engineering, Biology and Medicine* (Kadish, K., Smith, K. M., and Guilard, R., Eds.) pp 193−294, World Scientific Publisher, Singapore.

(51) Jiménez-Osés, G., García, J. I., Silva, A. M. G., Santos, A. R. N., Tomé, A. C., Neves, M. G. P. M. S., and Cavaleiro, J. A. S. (2008) Mechanistic insights on the site selectivity in successive 1,3-dipolar cycloadditions to meso-tetraarylporphyrins. *Tetrahedron 64*, 7937–7943.

(52) Maestrin, A. P. J., Ribeiro, A. O., Tedesco, A. C., Neri, C. R., Vinhado, F. S., Serra, O. A., Martins, P. R., Iamamoto, Y., Silva, A. M. G., Tomé, A. C., Neves, M. G. P. M. S., and Cavaleiro, J. A. S. (2004) A novel chlorin derivative of Meso-tris(pentafluorophenyl)-4-pyridylporphyrin: synthesis, photophysics and photochemical properties. *J. Braz. Chem. Soc. 15*, 923–930.

(53) Hao, E., Friso, E., Miotto, G., Jori, G., Soncin, M., Fabris, C., Sibrian-Vazquez, M., and Vicente, M. G. H. (2008) Synthesis and biological investigations of tetrakis(p-carboranylthio-tetrafluorophenyl)chlorin (TPFC). *Org. Biomol. Chem. 6*, 3732–3740.

(54) Hirohara, S., Obata, M., Alitomo, H., Sharyo, K., Ando, T., Tanihara, M., and Yano, S. (2009) Synthesis, photophysical properties and sugar-dependent in vitro photocytotoxicity of pyrrolidine-fused chlorins bearing S-glycosides. *J. Photochem. Photobiol., B 97*, 22–33.

(55) Hirohara, S., Obata, M., Alitomo, H., Sharyo, K., Ando, T., Yano, S., and Tanihara, M. (2009) Synthesis and photocytotoxicity of S-glucosylated 5,10,15,20-Tetrakis(tetrafluorophenyl)porphyrin metal complexes as efficient $^1O_2$-generating glycoconjugates. *Bioconjugate Chem. 20*, 944–952.

(56) Tanielian, C., Wolff, C., and Esch, M. (1996) Singlet oxygen production in water: aggregation and charge-transfer effects. *J. Phys. Chem. 100*, 6555–6560.

(57) Bonnett, R., and Martínez, G. (2001) Photobleaching of sensitizers used in photodynamic therapy. *Tetrahedron 57*, 9513–9547.

(58) Seybold, P. G., and Gouterman, M. (1969) Porphyrins XIII: Fluorescence spectra and quantum yields. *J. Mol. Spectrosc. 31*, 1–13.

(59) Vivanco, S., Lecea, B., Arrieta, A., Prieto, P., Morao, I., Linden, A., and Cossío, F. P. (2000) Origins of the loss of concertedness in pericyclic reactions: Theoretical prediction and direct observation of stepwise mechanisms in [3 + 2] thermal cycloadditions. *J. Am. Chem. Soc. 122*, 6078–6092.

(60) Tufariello, J. J., Mullen, G. B., Tegeler, J. J., Trybulski, E. J., Wong, S. C., and Ali, S. A. (1979) Synthesis in the tropane class of alkaloids. Pseudotropine and dl-cocaine. *J. Am. Chem. Soc. 101*, 2435–2442.

(61) Mishra, P. P., Patel, S., and Datta, A. (2006) Effect of increased hydrophobicity on the binding of two model amphiphilic chlorin drugs for photodynamic therapy with blood plasma and its components. *J. Phys. Chem. B 110*, 21238–21244.

(62) Drain, C. M., Gentemann, S., Roberts, J. A., Nelson, N. Y., Medforth, C. J., Jia, S., Simpson, M. C., Smith, K. M., Fajer, J.,

Shelnutt, J. A., and Holten, D. (1998) Picosecond to microsecond photodynamics of a nonplanar nickel porphyrin: solvent dielectric and temperature effects. *J. Am. Chem. Soc. 120*, 3781–3791.

(63) Obata, M., Hirohara, S., Tanaka, R., Kinoshita, I., Ohkubo, K., Fukuzumi, S., Tanihara, M., and Yano, S. (2009) In vitro heavy-atom effect of palladium(II) and platinum(II) complexes of pyrrolidine-fused chlorin in photodynamic therapy. *J. Med. Chem. 52*, 2747–2753.

(64) Boisbrun, M., Vanderesse, R., Engrand, P., Olié, A., Hupont, S., Regnouf-de-Vains, J.-B., and Frochot, C. (2008) Design and photophysical properties of new RGD targeted tetraphenylchlorins and porphyrins. *Tetrahedron 64*, 3494–3504.

(65) Gonsalves, A. M. d. A. R., Serra, A. C., and Pineiro, M. (2009) The small stones of Coimbra in the huge tetrapyrrolic chemistry building. *J. Porphyrins Phthalocyanines 13*, 429–445.

(66) Fox, S., and Boyle, R. W. (2006) Synthetic routes to porphyrins bearing fused rings. *Tetrahedron 62*, 10039–10054.

(67) Vicente, M. G. H., Nurco, D. J., Shetty, S. J., Osterloh, J., Ventre, E., Hegde, V., and Deutsch, W. A. (2002) Synthesis, dark toxicity and induction of in vitro DNA photodamage by a tetra(4-nido-carboranylphenyl)porphyrin. *J. Photochem. Photobiol., B 68*, 123–132.

(68) Zhang, X.-a., Lovejoy, K. S., Jasanoff, A., and Lippard, S. J. (2007) Water-soluble porphyrins as a dual-function molecular imaging platform for MRI and fluorescence zinc sensing. *Proc. Natl. Acad. Sci. U.S.A. 104*, 10780–10785.

(69) Morris, R. L., Azizuddin, K., Lam, M., Berlin, J., Nieminen, A.-L., Kenney, M. E., Samia, A. C. S., Burda, C., and Oleinick, N. L. (2003) Fluorescence resonance energy transfer reveals a binding site of a photosensitizer for photodynamic therapy. *Cancer Res. 63*, 5194–5197.

BC100356Z